



# Vibration-assisted electrochemical machining: a review

Hassan El-Hofy<sup>1</sup>

Received: 5 February 2019 / Accepted: 30 July 2019 / Published online: 12 August 2019  
© Springer-Verlag London Ltd., part of Springer Nature 2019

## Abstract

Electrochemical machining (ECM) uses a direct current (DC) at high density of 0.5–5 A/mm<sup>2</sup> which is passed through the electrolytic solution that fills the gap between an anodic workpiece and a pre-shaped cathodic tool. At the anodic surface, metal is dissolved into metallic ions and thus as the tool moves towards the workpiece at a constant feed proportional to the dissolution rate of the anodic surface, then its shape is copied into the workpiece. During ECM, the electrolyte is forced to flow through a narrow interelectrode gap at high velocity of more than 5 m/s to intensify the mass/charge transfer through the sublayer near the anodic surface. The electrolyte removes the dissolution by-products, e.g., hydroxide of metal, heat, and gas bubbles generated in the interelectrode gap. These machining by-products affect the process accuracy, efficiency, stability, and productivity. Ensuring the continuous flushing of these products is, therefore, essential. One of these methods is through the use of pulsed voltage. Introducing vibrational motion, at low or ultrasonic frequency, to the tool/workpiece or the machining medium became a viable alternative for the evacuation of the machining products during the vibration-assisted ECM (VA-ECM). Other attempts to further enhance VA-ECM performance include the proper tool design, addition of abrasive particles to the electrolyte medium, and use of magnetic flux assistance. This paper reviews the principles of VA-ECM, main research directions, process parameters, and performance indicators. Numerous fields of VA-ECM which include micro-slotting, micro-drilling, macro-drilling, electrochemical wire cutting (ECWC), polishing and finishing, and micro-tool fabrication have been covered. Several mathematical and statistical modeling and optimization techniques have been also examined. The current paper also outlines possible trends for future research work.

**Keywords** Vibration-assisted ECM · Material removal · Stability · Ultrasonic · Frequency · Amplitude · Current density

## 1 Introduction

The material removal in ECM is based on the principle of anodic dissolution according to Faraday's laws of electrolysis. ECM is used to machine complex shapes in conductive materials, which are difficult-to-machine by other conventional methods. The process is independent of the material hardness and toughness; it is burr and stress free with the advantages of achieving good surface quality and high material removal

rates (MRR). The process is adopted in forging dies, aerospace, automobile, electronics, and computer industries [1].

Controlling the part size and the machining stability, in ECM, is a difficult task because of the complex flow field in the interelectrode gap (IEG) which causes irregular anodic dissolution and lack of dimensional accuracy. The narrow machining gap accommodates a mixture of electrolyte, gas bubbles, and sludge which adversely affects the distribution of the current density, MRR, surface quality, and product accuracy. During normal ECM, the formation of a passive oxide layer on the workpiece surface stops the current flow through the IEG and negatively affects MRR, accuracy, and the process productivity. Proper evacuation of these products and the removal of the passive oxide layer are, therefore, necessary for ensuring improved process stability, accuracy, and efficiency. In order to achieve such goals, pulsed voltage and the vibration of the cathode/anode/electrolyte are applied in VA-ECM by many researchers. One of the most effective ways of increasing the accuracy of ECM is to use pulsed voltage of short durations. In order to improve the process performance,

---

Hassan El-Hofy is on leave from Alexandria University, Faculty of Engineering, Alexandria 21544, Egypt.

✉ Hassan El-Hofy  
hassan.elhofy@ejust.edu.eg

<sup>1</sup> Industrial and Manufacturing Engineering Department (IME), School of Innovative Design Engineering (IDE), Egypt-Japan University of Science and Technology (E-JUST), Alexandria 21934, Egypt

Rajkumar et al. [2] introduced the abrasive-assisted ECM for machining aluminum-boron carbide nanocomposite.

For increasing the process accuracy by reducing the IEG size, Davydov et al. [3] selected a proper electrolyte, used a gas-liquid mixture as an electrolyte, provided tool insulation, and applied a pulsed voltage. Using voltage pulses greater than 1 ms made it possible to machine with small IEG. Under such condition, the machining accuracy resulted from the reduction of the change of the electrolyte conductivity along that small gap which reduced the changes on shape errors. Moreover, a decrease of pulse time in the range of 1–100  $\mu$ s enhanced these effects which caused further accuracy improvement. Due to the smaller gap thickness associated with short pulses, the electrolyte temperature rise became more intensive which increased the electrolyte conductivity and machining at high current density became possible [4, 5].

The principles of ECM using ultrashort voltage pulses and the associated anodic dissolution localization issues were discussed by Skoczypiec [6] and Kumar et al. [7]. Ultrashort (nanosecond range) voltage pulses gave the possibility to achieve high localization of electrochemical dissolution (ECD) action. Under these conditions, the current density is determined by the activation overpotential and the dissolution process is driven by the periodic electric double-layer charging and discharging process. Moreover, the time of the double-layer charging to the activation overpotential depends on the gap thickness; therefore, the voltage pulse length can define the spatial resolution of machining. According to the Butler-Volmer equation (valid for active state of dissolution), the current density is exponentially related to the overpotential; therefore, a small change of the electrode potential leads to a large change of the current density; thus, additional effect of dissolution localization occurs [8]. Using ultrashort voltage pulses allowed machining of micro parts with an accuracy of less than 0.01 mm. Moreover, microstructures were also machined to 10- $\mu$ m depth, thus demonstrating the potential for the fabrication of high aspect ratio features using pulsed voltage [9].

VA-ECM is another alternative which has been adopted to improve the evacuation of the machining products from the IEG. Moreover, the ultrasonic (US) assistance can remove the passive oxide layer from the anodic surface. Consequently, the MRR, accuracy, and surface quality are improved. Figure 1 shows the main parameters that affect the quality of machined parts by the VA-ECM. These include factors related to electrode tool, vibrating element, electrolyte properties, applied voltage, and the vibration characteristics.

A large body of research has reported investigations regarding VA-ECM for understanding the process behavior and improving performance characteristics. Most of this work dealt with improving the process accuracy, surface quality, and process efficiency using experimental, mathematical modeling and optimization techniques. As shown in Fig. 2,

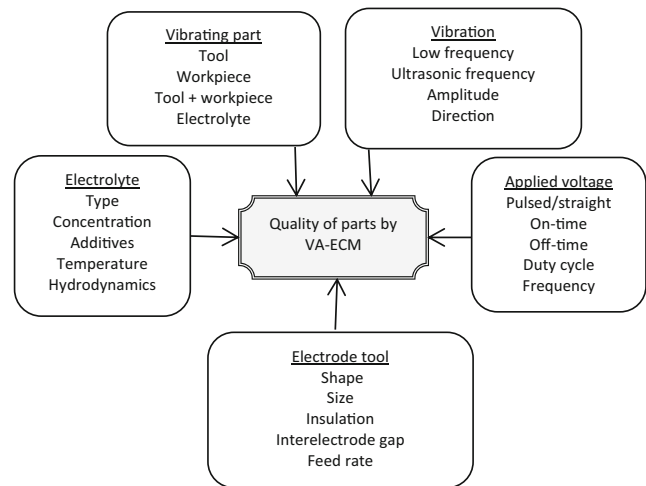


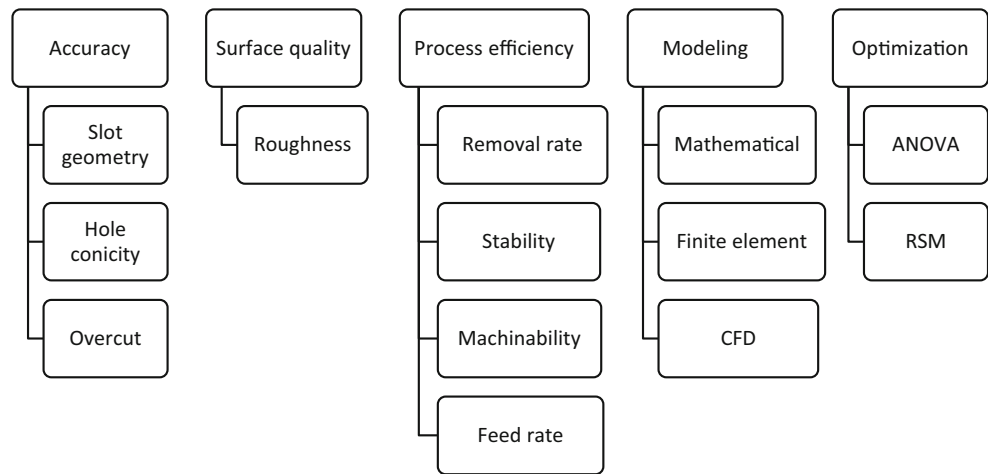
Fig. 1 Parameters affecting the quality of VA-ECM machined parts

the current review covers several ECM aspects such as surface roughness, product accuracy in terms of cut geometry, hole conicity, and overcut. Enhancing the process efficiency in terms of MRR, machining stability, machinability, and increasing feed rate is also covered. Statistical, mathematical, finite element method (FEM), and the computational fluid dynamic (CFD) models are also reviewed. Figure 3 shows the percentage of reviewer's coverage to the different VA-ECM performance indicators. Accordingly, 21% were concerned with enhancing MRR and 13% covered surface roughness or overcut. The current density or hole conicity was covered by 8% while each of the other issues related to accuracy, feed rate, and machining stability was covered by 6% of the researchers.

Figure 4 shows the percentage coverage of researchers to the frequency of vibration, type of voltage used, and the vibrating element during VA-ECM. It is evidently clear that 52% of work was conducted at low frequency of vibration while 48% of work was conducted using ultrasonic (US) frequency of vibration. The importance of using pulsed voltage is evident since it was implemented by 67% of researchers while 33% used the straight DC voltage. The majority of work was conducted using the cathodic tool vibration (67%), while workpiece vibration, combined workpiece and tool vibration, and the electrolyte vibration were implemented by 14%, 14%, and 5% of researchers respectively.

In this paper, the principles of VA-ECM are covered in Section 2. Micromachining applications including micro-slotting and micro-drilling are dealt with in Section 3. Drilling and wire cutting applications are covered in Sections 4 and 5 respectively. Polishing, finishing, and micro-tool fabrication are discussed in Section 6 while the process modeling and optimization techniques are presented in Section 7. A summary and outlook are dealt with in Sections 8 and 9 respectively.

Fig. 2 Review directions



## 2 Principles of VA-ECM

As manifested in Fig. 5, the oscillation movement of the workpiece is superimposed by its downward movement of the tool electrode. In the VA-ECM process, high amount of time is used for gap flushing; therefore, MRR is increased in comparison to normal ECM. Due to the high localization of the electrolytic dissolution action [4, 5, 8], vibration-assisted pulse electrochemical micromachining (VA-PECM) is applied for machining complex microstructures or precise machining of cutting tools or structured metal parts [10]. Figure 6 shows the effect of vibration amplitude on the gap size for a given frequency and minimum gap size [11].

Skoczypiec [12] analyzed the electrolyte flow through the gap in the US-assisted ECM (USECM) at 20-kHz frequency and less than 10- $\mu$ m amplitude. He proved that the US vibration changed the dissolution process in IEG such that the machined allowance and the MRR were increased.

Generally, the US vibration enhanced the removal of heat and reaction products out of the machining zone. It supported the diffusion process, decreased the rate of passivation, changed the coefficient of electrochemical machinability (current efficiency  $\times$  conductivity) and created optimal hydrodynamic conditions from the surface layer point of view [12].

During USECM, the US waves created cavitation microbubbles near the workpiece surface. Moreover, in the area adjacent to the electrode surface, micro-jets with high velocity ( $10^2$  m/s) were also created which gave the possibility of intensification of mass, electric charge, and heat transfer, leading to the increase in the electrochemical dissolution rate. These phenomena were useful when the passivation layer was created during ECM. Such a layer was removed by using the high pulse pressure ( $10^2$  MPa) created by the US vibration [13, 14]. In this regard, Ruszaj et al. [15, 16] conducted primary investigation of EC micromachining supported by US vibration at 22 kHz and amplitude 16  $\mu$ m and concluded that

Fig. 3 Performance indicators covered by researchers

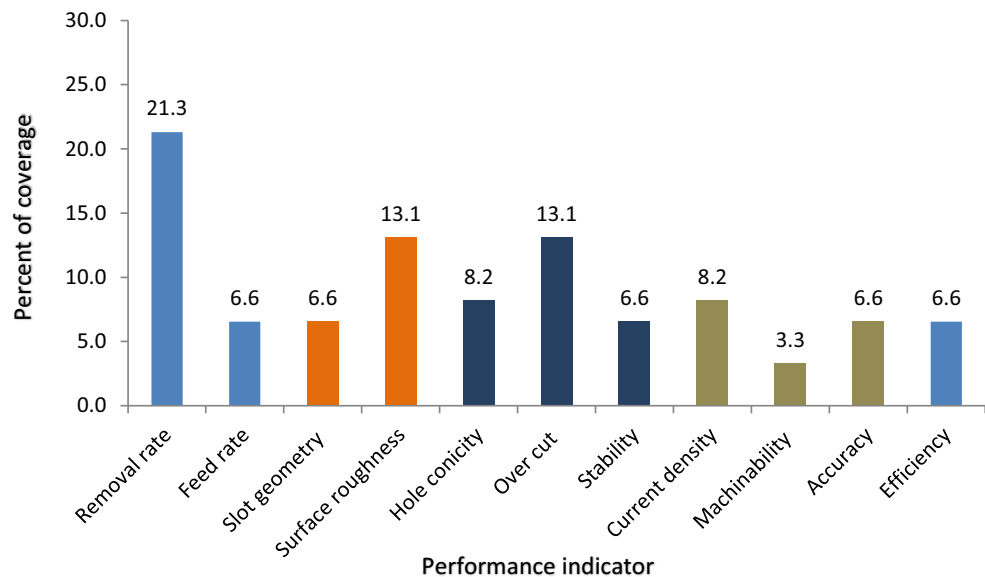
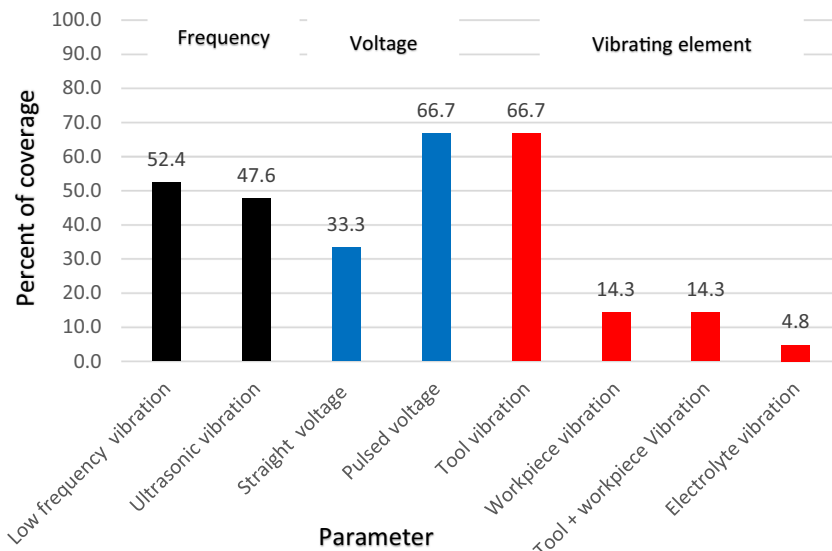


**Fig. 4** Parameters covered by researchers



the US vibration decreases the surface roughness parameter, *Ra*, compared with the classical ECM process. They summarized the effect of US in ECM as follows:

- Supports diffusion and decreases the rate of passivation.
- Decreases the potential drop in the layers adjacent to electrodes.
- Increases the coefficient of electrochemical machinability.
- Creates optimal hydrodynamic conditions for good surface layer quality.

In a further work by Skoczypiec [17], it was reported that the use of combination of synchronized low-frequency pulsed voltage and an oscillating and feeding electrode enabled machining with small IEG in the range of 10–50 μm and significantly higher current densities. At minimum gap thickness, the voltage was switched on for 500–5000 μs leading to the material removal process. Under such conditions, low amount of electrolyte was transported through the IEG. When the gap was maximized, a large amount of electrolyte was supplied to the IEG, thus flushing away the machining products. Rajurkar

**Fig. 5** Variation of gap size in one period of time [10]

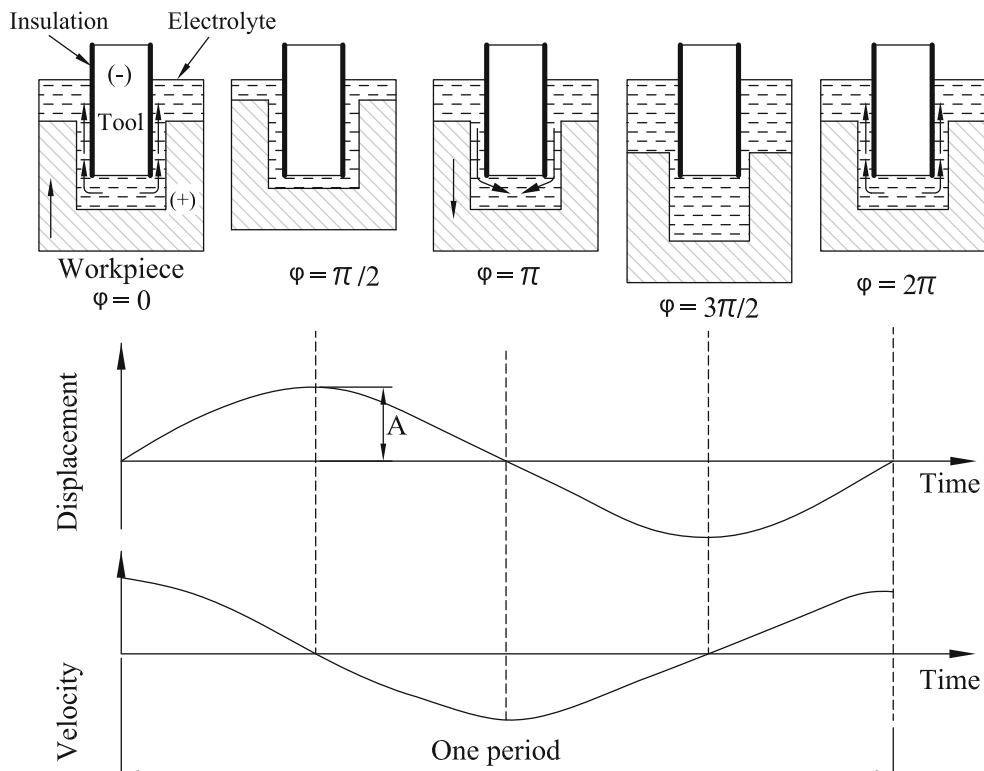
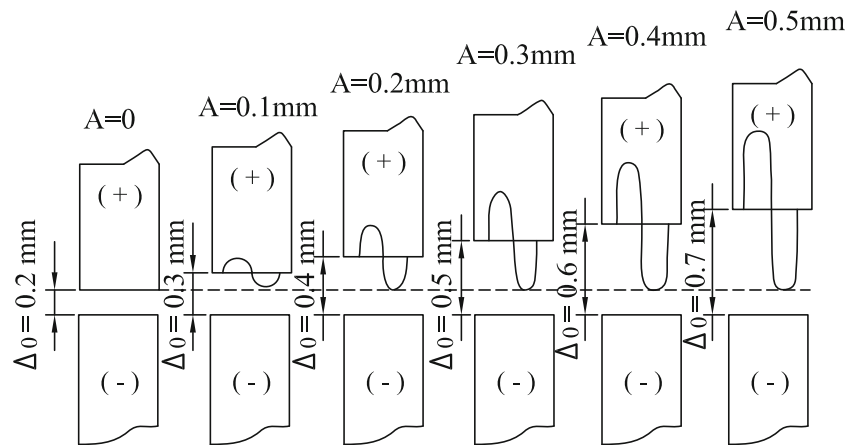


**Fig. 6** Variation of interelectrode gap with vibration amplitude at fixed initial gap [11]



and Zhu [1] developed a precision ECM process using an eccentric orbital workpiece movement with traditional ECM. Their theoretical and experimental analyses indicated that adding the orbital motion to ECM distributed the electrolyte flow more uniformly and, hence, caused a significant reduction in the flow field disrupting phenomena that adversely affected machining accuracy. The proposed method offered substantial gains in the process accuracy and the uniformity of the machined components. In a further work, Hewidy et al. [18] proposed the cathodic tool orbital motion technique to enhance the ECM accuracy and eliminate the presence of the central spikes. On the other hand, Sadollah and El-Hofy [19] used the orbital ECM technique to remove the protrusions formed in EDM machined surfaces. Paczkowski et al. [20] machined curvilinear slots using shaped tool electrodes, vibrating at frequency of 30 Hz and amplitude of 0.1 mm in the longitudinal direction and 0.05 mm in the traverse direction.

The distribution of gas, sludge, and temperature in the IEG affects the electrolyte conductivity and determines the machining accuracy in ECM. In order to improve the heat transfer, MRR, and surface profile, Fang et al. [21] and Zeng et al. [22] adopted the technique of the pulsating electrolyte supply as shown in Fig. 7. Their experimental results showed that the MRR and surface profile were enhanced using such a technique [21].

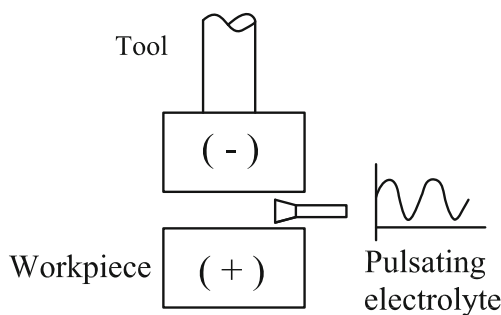


**Fig. 7** Pulsating electrolyte configuration [21]

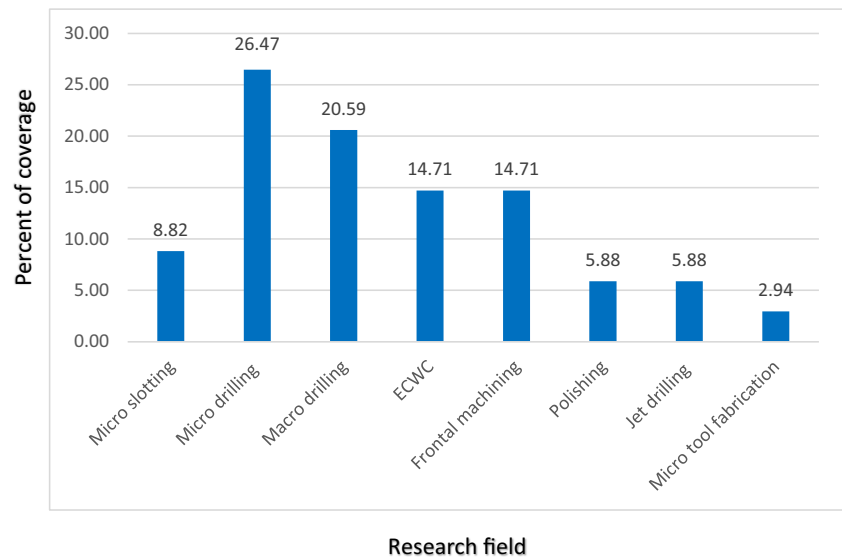
Numerous fields of VA-ECM have been covered by many researchers. These areas include micro-slotting [11, 23, 24], micro-drilling [10, 25–32], macro-drilling [33–39], electrochemical wire cutting (ECWC) [40–45], polishing and finishing [46, 47], and micro-tool fabrication [48] as shown in Fig. 8. Modeling and optimization were covered by many researchers [11, 12, 20, 21, 23, 24, 26, 35–43, 45, 49–54]. The summary of the vibration-assisted ECM (VA-ECM) conditions, machining variables, and performance indicators are shown in Table 1.

### 3 Micromachining

Electrochemical micromachining (EMM) is gaining importance in slotting and drilling of holes due to its advantages that include no tool wear, high MRR, absence of burrs, and its ability to produce complex shapes irrespective of workpiece hardness.

**Micro-slotting** When fabricating micro-slots, high flow resistance occurs with the increase of the slot length. Material hydroxide and other machining products accumulate in the outlet of the electrolyte which limits the maximum possible feed rate of the cathodic tool electrode. In order to solve such a problem, Xiaochen et al. [23] and Jia et al. [54] proposed the idea of flow channel contraction using a cathodic tool with variable cross section to machine micro-slots of  $300 \pm 30 \mu\text{m}$  depth and 60 mm length in stainless steel. Such a contraction increased the electrolyte flow velocity along the IEG and flushed away the machining by-products. Moreover, the addition of the cathodic tool vibration, at low frequency of 10 Hz and 0.3-mm amplitude, enhanced the electrolyte flushing process, doubled the feed rate, and ensured the uniformity of the machined slots. Furthermore, Feng et al. [11] fabricated microslot arrays of complex shapes, using the traditional ECM, which suffered from poor stability and low machining accuracy. However, the addition of low-frequency vibration to

**Fig. 8** Research fields of VA-ECM



ECM improved the process stability while the average slot width and slope were decreased by increasing the vibration amplitude and frequency. In a further work, Goshal et al. [24] generated various cross-sectional profiles using different micro-tool shapes. Their results showed that vibrating the micro-tool with  $0.3\ \mu\text{m}$  and low frequency of 85 Hz improved the surface finish. Such an observation was related to the transient bubble collapse and, moreover, the impact of energetic micro-jets on the anodic surface which caused the effective flushing of the machining products from the IEG [13, 14].

**Micro-drilling** Micro-hole drilling at high aspect ratio is a challenge in EMM due to the difficulty of removal of the machining products from the IEG. In this regard, Goshal et al. [25] studied the effect of vibration (82 Hz and  $3\ \mu\text{m}$  amplitude) of micro-tool, using pulsed voltage (3 MHz), micro-tool shape, and workpiece thickness on the aspect ratio of micro features in EMM of SS 304. They found that the use of low-frequency vibration made the electrolyte flow easier and, slightly, increased the overcut due to the higher current density. The same authors [26] investigated the effect of gap voltage (3–6 V), pulse frequency up to 10 MHz, vibration amplitude  $0.3\text{--}3\ \mu\text{m}$ , and frequency 200–963 Hz of tool vibration on the overcut of drilled micro boreholes in SS 304 workpiece. Their results showed the increase of the average current with the increase of vibration amplitude caused the collapse of the gas bubbles and enhanced mass transfer and coefficient of diffusivity which, in turn, increased the current density. The average current showed an increase with frequency up to 500 Hz beyond which stable microbubbles were formed which reduced the electrolyte conductivity and the current density. They reported the increase of overcut with increasing both the vibration amplitude and frequency. Low vibration amplitude and medium frequency of vibration of the micro-

tool provided an easy electrolyte supply to the narrow micromachining zone, thereby improving both the shape control and surface quality [26]. An attempt was also made for evacuating the electrolyte from the IEG through the use of the proper tool design by Yang et al. [27] who drilled micro-holes in  $300\text{-}\mu\text{m}$  SS 304 using cylindrical and semi-cylindrical rotating tools, vibrating at frequency of 40 kHz, and  $4\text{-}\mu\text{m}$  amplitude. Consequently, the use of semi-cylindrical tools increased the flow space and permitted drilling holes to a depth of  $300\ \mu\text{m}$  which was difficult to achieve using cylindrical tools without US vibration. Moreover, the use of US vibration improved electrolyte diffusion and convection as well as the gas bubbles dispersion which, in turn, saved a considerable machining time, increased MRR and improved the machining accuracy. During micro-hole drilling, at different feed rates, Feng et al. [28] concluded that the combination of high vibration frequency of 50 Hz and low amplitude of  $5\ \mu\text{m}$  achieved higher MRR than that at low frequency of 10 Hz and high amplitude of  $25\ \mu\text{m}$ .

Moreover, Wang et al. [32] used cylindrical and disk-shaped cathodic tools for micro-hole drilling with and without tool vibration. Accordingly, the disk micro-tool electrode focused the electric field on the anode and improved the dissolution localization. When the US vibration was added to the disk tool, the machining speed as well as the maximum depth of the micro-holes were increased and the taper and hole diameter decreased while the surface quality was improved compared with that of micro-hole drilling without US tool vibration.

During normal ECM, a passivation problem arises which stops the flow of the electrolyzing current and negatively affects MRR and the process productivity. The introduction of US vibration to the electrolytic cell, immersed in US bath, was used for controlling passivation problem. In this regard,



**Table 1** Summary of V-ECM operations, conditions, and performance indicators

Reference	Process	Vibration		Voltage			Variables	Performance indicators
		Vibrating element	Amplitude (µm)	LF (Hz)	US (kHz)	Straight (V)		
Feng et al. [11]	Micro-slotting	W	0–500	0–50	–	–	Frequency-amplitude-initial gap	Stability-slot shape
Xiaochen et al. [23]		T	300	10	20	–	Flow field-cathode shape	Feed rate-slot shape
Goshal et al. [24]		T	300	85	–	3	Electrolyte concentration Tool shape	Roughness-overcut
Liu, et al. [10]	Micro-drilling	W	3–14	0–200	–	6	Amplitude-frequency	MRR-side gap
Goshal et al. [25]		T	3	82	–	3	Tool shape-workpiece thickness Voltage frequency	Stability-overcut Aspect ratio-taper
Goshal et al. [26]		T	0.3–3	200–963	–	3–6	Pulsed voltage-tool amplitude Vibration frequency	Current density-overcut
Yang et al. [27]		T	4	–	–	7.12	Tool shape-US vibration	MRR-precision
Feng et al. [28]		T	5–25	10–50	–	20–40	Vibration frequency-amplitude Feed rate-WP composition-peak current	MRR
Kurogi et al. [29]		T	4	–	63	10	Electrolyte concentration	Accuracy
Wang et al. [30]		W	0–5	–	28	7–16	Electrolyte concentration-amplitude-gap voltage	Accuracy-overcut-stability
Wang, et al. [32]		T	0–15	–	28	–	Feed rate-vibration amplitude	Taper-roughness-overcut
Wang et al. [45]		T	6–12	10–200	–	–	B <sub>4</sub> C concentration-time-frequency	Roughness
Goel and Pandey [50]	Jet drilling	M	On-time 0–1.2 s	–	–	0–600	Voltage-interelectrode gap-electrolyte concentration-electrolyte pressure-pulse on-time Current density-original surface condition	MRR-taper
Mitchell-Smith and Clare [55]		W	–	–	–	–	–	Kerf width-aspect ratio-roughness
Patel et al. [33]	Drilling	M	0,15, 36	–	–	22, 26	US amplitude-pulse frequency-peak current-time	Surface roughness-hole taper
Natsu et al. [34]		T	4x20 z	–	32x,45z	10	Feed rate-complex vibration	Speed-accuracy
Ebeid et al. [35]		T	20–100	50	12–24	–	Vibration amplitude-feed rate-back pressure-gap voltage	Overcut-hole conicity
Jadhav et al. [36]		T	16–20	–	US	16–20	Ultrasonic on-time/off-time-voltage-pulse on-time	MRR Overcut
Ayyappan et al. [37]		T	50	–	15–25	–	Electrolyte concentration-gap voltage-frontal gap	MRR-roughness
Hewidy et al. [38]		T	0–200	50	12	–	Vibration amplitude	MRR-current density-electrolyte pressure
Zou et al. [40]	ECWC	T	10	0.5–2.5	–	18	Vibration frequency-amplitude-feed rate	Feed rate-slit width-efficiency
Xu et al. [41]		T + W	1	0–500	–	5–10	Electrolyte concentration-vibration amplitude-feed rate-pulse period/duration	Slit width/homogeneity
Fang et al. [43]		T	7500	1.5	–	18	Ribbed wire-large amplitude	MRR-efficiency
Jiang et al. [44]		T	1–15	–	20–90	25–39	Frequency-amplitude-B <sub>4</sub> C concentration-voltage	Max feed rate Surface quality

Table 1 (continued)

Reference	Process	Vibration		Voltage			Variables	Performance indicators
		Vibrating element	Amplitude ( $\mu\text{m}$ )	LF (Hz)	US (kHz)	Straight (V)		
Wang et al. [45]		W	0–50	0–100	–	–	4	Stability-overcut-accuracy
Kim and Park [46]	Polishing	M	–	–	28	7	–	Roughness
Pa [47]	Finishing	M	–	–	46	–	–	Roughness
Ghoshal and Bhattacharyya [48]	Micro-tool fabrication	W	1.5–6	232	–	2–10	–	MRR-diameter

Nicoara et al. [51] studied the evolution of current, voltage, and electrolyte temperature during US-assisted ECM at frequencies of 20 kHz and 50 kHz. Their results showed the increase of anode potential and the current density which, in turn, reduced the deteriorating effect of passivation layer and increased the MRR by 1.6%.

One way of removing the insulating passivating layer formed during machining WC and SS 304 by ECM is to apply the US vibration to the tool electrode. Such a layer is known to disturb the current flow between the cathodic tool and the anodic workpiece electrodes and, moreover, affects the machining accuracy. In this regard, Kurogi et al. [29] used US tool vibration at 43 kHz and 4–7- $\mu\text{m}$  amplitude at low electrolyte concentration (10%  $\text{NaNO}_3$ ) and pulsed current source (10 V). They concluded that the replicating accuracy was improved while the machining speed was decreased. Using such a technique, machining of WC became possible by applying the US vibration to the electrode tool.

Liu et al. [10] drilled micro-holes in SS 321 using vibration amplitude of 3–14  $\mu\text{m}$ , a frequency of 0–200 Hz, a pulsed voltage of 6 V with 50% duty cycle, and a frequency of 2 kHz. Their results revealed that the amplitude of 3–14  $\mu\text{m}$  and low frequency of 50–200 Hz influenced MRR significantly. The lower the frequency, the more was the improvement in MRR that reached its maximum at 50 Hz and 12- $\mu\text{m}$  amplitude. On the other hand, the smallest side gaps were achieved at an amplitude range of 4–7  $\mu\text{m}$  and frequency between 50 and 200 Hz. Wang et al. [30] concluded that the increase in workpiece vibration amplitude is beneficial for excluding the reaction products from the IEG (Fig. 9). Consequently, the machining was stable when the vibration amplitude was beyond a certain value; henceforth, the machining accuracy changed little with the increase in vibration amplitude.

The introduction of abrasive particles into the electrolyte was considered as an effective technique for enhancing the performance of VA micro-ECM by Jiang et al. [44]. In this line, Wu et al. [31] combined VA micro-ECM with polishing for machining 3D microcavities by using an electrolyte containing suspended  $\text{B}_4\text{C}$  abrasive particles. Accordingly, the electrochemical reaction by-products were effectively removed by the abrasion action of the  $\text{B}_4\text{C}$  particles which ensured efficient and stable micro-ECM process.

It is noteworthy to say that during micromachining, the use of proper tool design together with the application of US vibration increase MRR and the drilling speed and improves the process accuracy while the application of low-frequency vibration improves the surface quality of VA-ECM. The use of US vibrations helps in flushing away the machining products from the IEG and stops the formation of the passive layer on the anodic surface which enhances the ECD action. Moreover, the addition of abrasive particles to the electrolyte medium ensures efficient and stable drilling by VA-ECM.



## 4 Drilling

Researchers have been investigating techniques of enhancing the ion transport in the IEG to improve the MRR and quality of machined parts by ECM. It is well known that the use of pulsed voltage improves the dimensional accuracy by reducing the electrolyte temperature. It allows better opportunity to flush away the machining products from the IEG. Moreover, the use of low-frequency vibration of the workpiece/tool enhances electrolyte flushing while the US vibration breaks the agglomerated by-products on the anodic surface and, therefore, is adopted to enhance the removal of such products in ECM. In this regard, Natsu et al. [34] investigated the effect of the direction and amplitude of US vibration on the machining speed and the replicating accuracy of holes drilled by USECM. They concluded that applying the US vibration improved the replicating accuracy and increased the drilling speed. The complex vibration regime, shown in Fig. 10, had more significant effect on both the accuracy and drilling speed compared with the individual lateral vibration regime.

Ebeid et al. [35] addressed the improvement of the machining accuracy in ECM drilling by adding low-frequency (50 Hz) vibration to the tool electrode at an amplitude of 0–100  $\mu\text{m}$ , applied voltage (12–24 V), feed rate (0.6–1.4 mm/min), and back pressure. They concluded that the amplitude of tool vibration was the most significant parameter on the accuracy of VA-ECM. However, this effect was diminished after reaching the amplitude of 80  $\mu\text{m}$ . Moreover, the introduction of low frequency of vibration improved the produced accuracy by 15% while the conicity of holes was reduced by 23%. Furthermore, Jadhav et al. [36] investigated the effect of voltage pulse on-time, US vibration on-time and off-time, and amplitude on both MRR and overcut. Accordingly, the maximum MRR was achieved at 16 V, pulse on-time 500  $\mu\text{s}$ , US on-time 2 s, US off-time 8 s, and vibration amplitude 18  $\mu\text{m}$ . On the other hand, the minimum overcut was obtained at 18 V, pulse on-time 150  $\mu\text{s}$ , US on-time 4 s, US off-time 9 s, and vibration amplitude 20  $\mu\text{m}$ .

Researchers have attempted to enhance the performance of VA-ECM by introducing the concept of a low-frequency

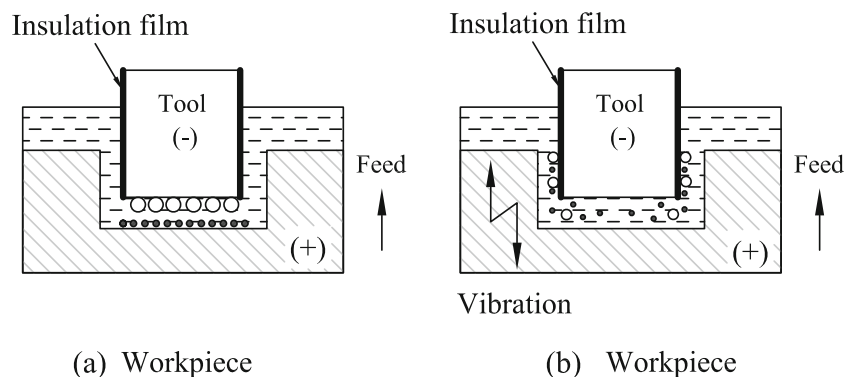
vibrating tool assisted by a magnetic flux (Fig. 11) as an efficient hybrid technique in ECM [37]. Their results indicated that the magnetic flux-assisted vibrating tool increased MRR from 10% to 96%. Such an increase was related to the fact that the magnetic flux facilitated and drove the sludge out of the IEG. Consequently, the current density was increased due to the movement of ions triggered by the magnetic flux, which assured the increase of MRR. A slight increase in surface roughness parameter,  $Ra$ , was also noted in comparison to machining with the NaCl electrolyte alone [37].

Embedding US waves in the fast-flowing electrolyte is more practical than vibrating a large tool or workpiece electrode. In this context, Patel et al. [33] combined the pulsed current and ultrasonic wave with the flowing electrolyte through the tubular electrode (shown in Fig. 12) to drill deep holes in 6061-T6 aluminum. Such a combination enhanced the part quality by reducing the surface roughness parameter  $Ra$  from 2.5 to 1  $\mu\text{m}$  and the taper angle of the drilled holes from 11 to 1° at the expense of MRR. At large US power, the high impacting velocity of micro-jets on the anodic surface reduced MRR, increased surface roughness, and caused micro-pitting.

Ultrasonic-assisted jet electrochemical micro-drilling (Jet-ECMD) is a variation of ECM used by Goel and Pandey [50] who combined US vibrations with the electrolyte jet, as shown in Fig. 13. They concluded that the maximum increase in MRR of 83.50% was obtained at pulse on-time of 1.2 s while the minimum hole taper was found to be 0.38°. Moreover, Mitchell-Smith and Clare [55] added that the use of US assistance enhanced the aspect ratio of machined grooves by Jet-ECMD due to the reduction of the passivating layer formation by 23% (Fig. 14). Under such conditions, a larger area of the groove was affected by the high current density which was increased subsequently from 2% without US assistance to 22% with US vibration, thus reducing  $Ra$  by 31%.

In summary, the use of complex US vibration improves the process accuracy and the drilling speed. Adding a magnetic field to VA-ECM increases current density, MRR, and surface roughness. Adding US vibration to the flowing electrolyte decreases the surface roughness parameter,  $Ra$ , and produced

**Fig. 9** Effect of workpiece vibration on the hydrogen bubbles and sludge evacuation. **a** Without vibration and **b** with vibration [30]



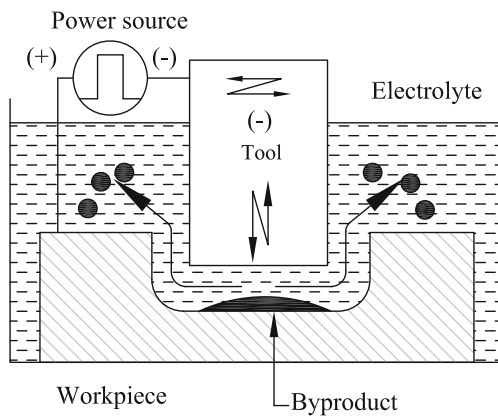


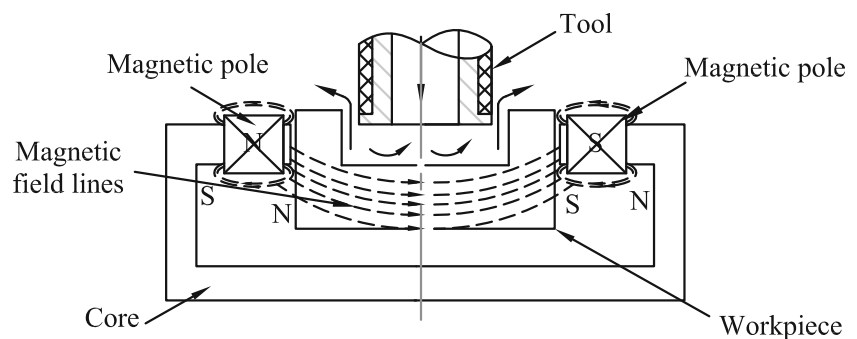
Fig. 10 Complex tool vibrations [34]

hole conicity. The use of US jet drilling increases MRR and the process accuracy and improves the surface quality.

## 5 Wire ECM

The diffusion of electrolytic dissolution products such as gas bubbles was difficult in normal wire EMM which, in turn, caused poor homogeneity of slit width and large edge radius. These bubbles were driven out of the machining gap by using the low-frequency vibration during VA-WECM. In this context, Zou et al. [40] used an axial vibrating wire electrode (1.5 Hz and 10  $\mu\text{m}$  amplitude) to improve the mass transfer in VA-WECM. The particle tracing simulation showed that the recycling of the electrolyte and the removal of dissolution products were promoted as shown in Fig. 15b, compared with the smooth nonvibrating wire electrode (Fig. 15a). However, the use of ribbed wire structure (Fi. 15c) created a pulsed current from the straight DC voltage. The results showed the reduction of the slit width and the increase of feed rate in the case of the ribbed wire compared with the smooth vibrating wire. Moreover, the high vibration amplitude increased the slit width while the frequency showed a minor effect. Que et al. [42] integrated pulsed ECM and a reciprocal travelling wire electrode to improve the process accuracy and stability.

Fig. 11 Interaction of magnetic flux lines with tool and workpiece [37]



For further enhancement of the electrolyte renewal during wire ECM, Fang et al. [43] applied low vibration frequency of 1.5 Hz and large amplitude of 7.5 mm to the ribbed wire (Fig. 16). The use of large amplitude intensified the bubble removal process in both upward and downward durations. Consequently, the MRR and the machining efficiency were enhanced by 25% and 22% respectively compared with the vibrating smooth wire. Furthermore, Xu et al. [41] concluded that the large amplitude (0.5 mm) and the high speed of wire vibration and the large amplitude and high frequency of work-piece vibration reduced the edge radius and improved the homogeneity of the slit width (Fig. 17).

Using a wire electrode with micro-diameter was adopted to reduce the overcut and improve the machining accuracy of microwire ECM by Wang et al. [45] who developed a wire electrochemical micromachining system with micro-tool vibration unit. They concluded that the low frequency and small amplitude of vibration significantly improved the process stability, overcut, machining accuracy, and precision of micromachined parts. Furthermore, Jiang et al. [44] added  $\text{B}_4\text{C}$  particles to the  $\text{NaNO}_3$  electrolyte during machining microgrooves in VA-ECWC. They concluded that adding  $\text{B}_4\text{C}$  particles significantly reduced the electrolytic products deposited on the wire electrode surface, prevented bubbles from accumulating in the IEG, and, consequently, improved the surface quality of the microgrooves.

In brief, high MRR and improved process efficiency can be achieved by using a smooth or ribbed wire vibrating at low frequency. Adding abrasive powder to the electrolyte during VA-WECM improves the surface quality.

## 6 Polishing, finishing, and micro-tool fabrication

Kim and Park [46] introduced the US vibration to study its effect on the surface roughness, MRR, and the productivity during vibration-assisted electrochemical polishing (VECP). They reported the enhancement of the surface smoothing effect and the process ability which limited the occurrence of surface pitting and reduced surface roughness. Pa [47] conducted

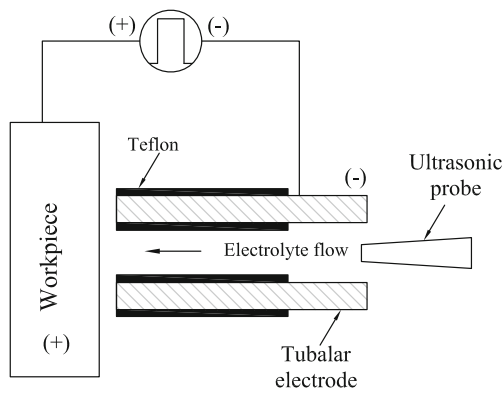


Fig. 12 VA-ECM using US waves to the flowing electrolyte [33]

electrochemical finishing of cylindrical turned surfaces for die materials using a specially designed tool shape. When the small end radius cylindrical tool was replaced by a plate-shaped tool, the electrolytic machining products and heat were removed more rapidly and produced higher surface quality. Additionally, by adding the US vibration to the plate-shaped tool, the discharging of dregs, from the IEG, was further enhanced which improved the surface quality of the final products. VA-ECM was further adopted for the fabrication of tungsten micro-tools, vibrating at low frequency of 232 Hz and small amplitude of 1.5–6  $\mu\text{m}$  [48]. Accordingly, uniform diameters of tungsten micro-tools were produced by controlling the diffusion layer thickness within a very short time by introducing the low-frequency vibration of the micro-tool.

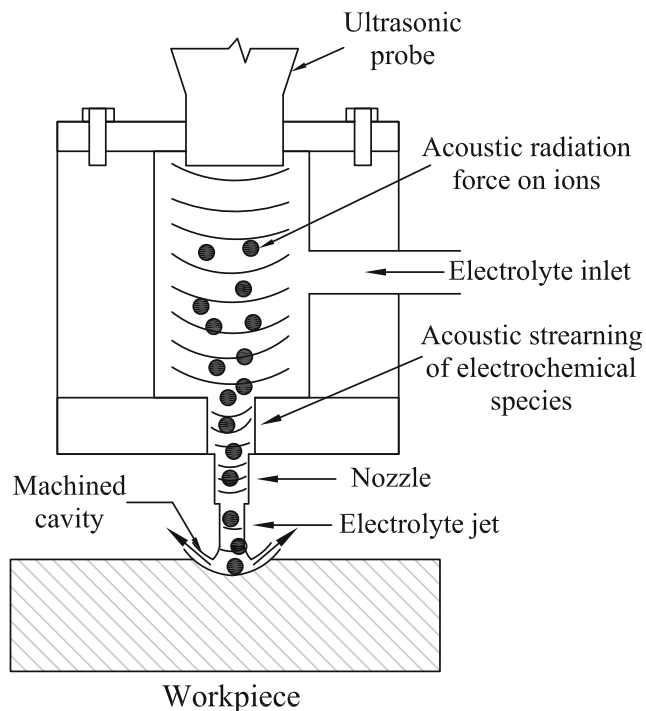


Fig. 13 Ultrasonic assisted jet electrochemical micro-drilling [50]

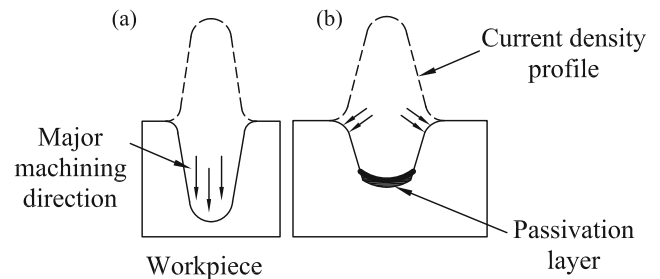
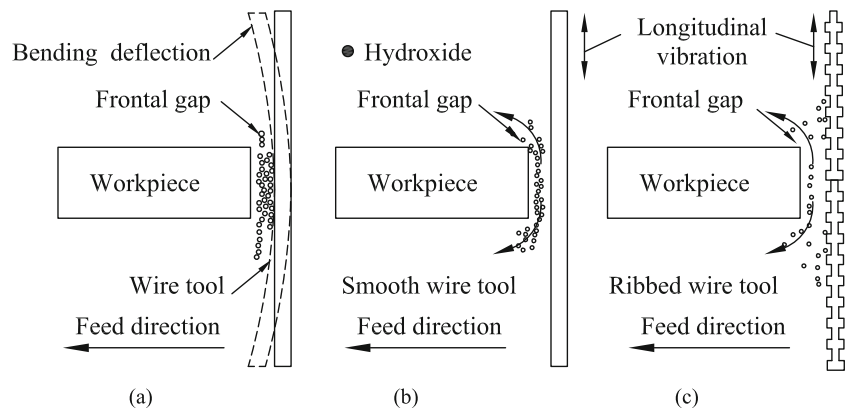


Fig. 14 Effect of US vibration on the cut profile. a With UA and b without UA [55]

## 7 Modeling and simulation

Several attempts have been made to model the electrolyte flow and material removal mechanism and to optimize the process conditions towards minimizing overcut, slot width and taper, maximizing the MRR and enhancing the machining productivity and surface quality. Ghoshal et al. [26] introduced an electrical circuit mathematical model of EMM and investigated the effects of pulsed voltage (3–6 V) and 10 MHz, tool vibration amplitude (0.3–3  $\mu\text{m}$ ), and vibration frequency of 200–963 Hz on the current density and overcut. Results showed that the experimental MRR was in good agreement with the theoretical analysis. Hewidy et al. [38] established a mathematical model to assess the mechanism of metal removal for EC drilling assisted by a low-frequency vibration of 59 Hz and 0–200- $\mu\text{m}$  amplitude. They reported that the variation of the gap pressure removed the machining products and allowed the renewal of the electrolyte in IEG. Moreover, the reciprocal motion between the tool and the workpiece surface enhanced the circulation of the electrolyte through the interface thus permitting higher current densities which improved the quality of the machined surface. Their analytical model revealed that there was a complexity in relating the tool vibration amplitude and the equilibrium gap size, because it caused tool damage. Wang et al. [45] developed a mathematical model for overcut in wire electrochemical micromachining with micro-tool vibration unit. The influence of micro-tool vibration on the processing stability, overcut, and machining accuracy of microwire electrode electrochemical cutting was investigated. For the purpose of improving the precision and stability of ECM of curvilinear surfaces using a vibrating tool, a mathematical model with regard to electrolyte flow hydrodynamics was developed by Paczkowski et al. [20]. They presented a system for controlling and monitoring ECM in a way that it allowed a suitable modification of parameters related to the frequency of tool vibrations and tool design stage verification as well as optimization of machining behavior. An equation relating the dynamic voltage caused by a vibrating tool electrode and performance variables was deduced. Using this equation, the dynamic voltage and its variables, along with system parameters, were investigated by Lihong et al. [52]. Their results showed that this technique significantly increased the machining localization of the electrochemical micromachining.

**Fig. 15** Distribution of machining products in ECWC. **a** Smooth wire without vibration, **b** smooth wire with vibrations, and **c** ribbed wire with vibrations [40]

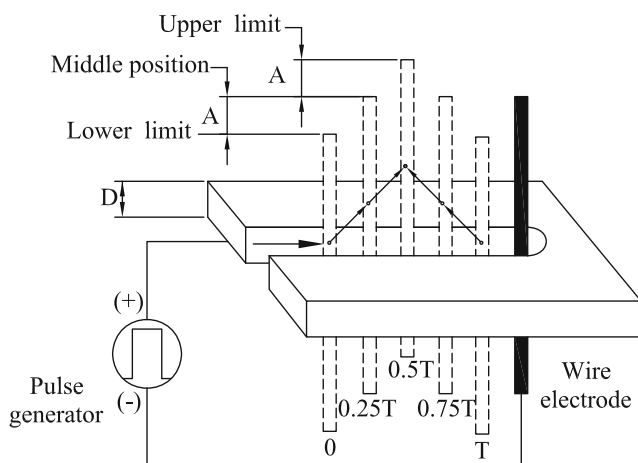


Ghoshal et al. [24] presented simulation models for the current density distribution along the side wall and top and bottom surfaces during blind microchannel generation in SS304 using different tool shapes and  $H_2SO_4$  electrolyte concentrations of 0.5–0.3 M. A pulsed voltage of 3 V, and 5 MHz and vibrating tool at low frequency of 85 Hz and 0.3- $\mu\text{m}$  amplitude were employed in order to predict the shape of cross section of the machined profiles. Fang et al. [21] presented a multi-physics model coupling of electric, heat, transport of diluted species, and a pulsating fluid flow (Fig. 6) had a significant impact on the distributions of velocity, gas fraction, and temperature near the workpiece surface along the flow direction which improved the surface quality. Xu et al. [41] presented another simulation study of the electric field for the wire and workpiece vibration conditions, electrolyte properties, and feed rate on the standard deviation of the slit width and edge radius. The flow field simulation of Fang et al. [43] revealed that the gas bubbles were expelled effectively from the IEG as the wire electrode moves upward in a large amplitude of 7.5 mm and low frequency of 1.5 Hz. Zou et al. [40] used the particle tracing simulation which showed that the recycling of the electrolyte and the removal of dissolution products were promoted in case of

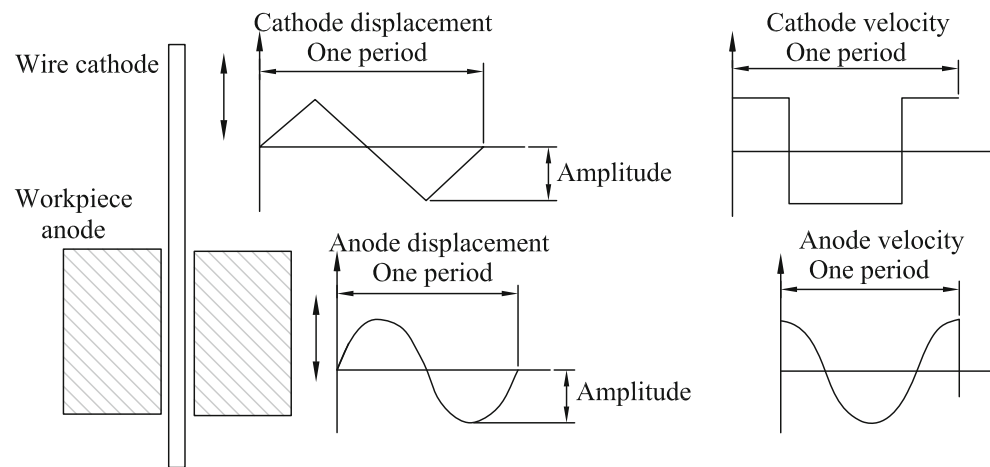
using ribbed wire compared with the smooth wire electrode.

Skoczypiec [49] applied the CFD and FEM for the analyses of electrolyte flow through the gap in USECM using a vibrating tool electrode (20 kHz and 2–8- $\mu\text{m}$  amplitude) normal to the electrolyte velocity component. The work analyzed the multiphase, turbulent, and unsteady flow between anode and cathode, under the assumption that the cavitation phenomenon occurred. Presented results proved that the US application changed the condition of dissolution process in IEG such that the machined allowance and MRR were increased by 75% and 80% respectively at interelectrode gap voltage of 20 V. On the other hand, Skoczypiec [12] analyzed the electrolyte flow through the gap in USECM using the CFD method at 20-kHz frequency and amplitude less than 10  $\mu\text{m}$  in order to predict the distribution of cavitation bubbles along the gap. Numerical investigation revealed that the intensity of cavitation affected the conditions of the dissolution process which depends on the amplitude of US vibration. He reported improvement of current density, MRR, machining allowance, and machinability. In the same line, Feng et al. [11] studied the effect of flow pattern and pressure on the flow field stability using the CFD simulation. They concluded that the low-frequency oscillation-assisted ECM by improving the machining stability.

Based on the FEM, Wang et al. [32] compared the cylindrical and disk-shaped cathode tools during micro-hole drilling at different feed rates with and without tool vibration. Their results revealed that the disk micro-tool electrode focused the electric field on the anode and improved the dissolution localization. Accordingly, the US vibration increased the feed rate and penetration depth, decreased the taper and diameter, and improved the surface quality of the machined holes. Xiaochen et al. [23] used the same method for numerical simulation of the flow field in ECM. Accordingly, the addition of the cathodic tool vibration, at low frequency of 10 Hz and 0.3-mm amplitude, enhanced the electrolyte flushing process, doubled the feed rate, and ensured the uniformity of the machined slots. Liu et al. [39] developed a three-dimensional model of flow field in ANSYS CFX software



**Fig. 16** VA-ECWC with large amplitudes [43]

**Fig. 17** VA-WECM using wire and anode vibrations [41]

for a rotating and vibrating cathode. Their simulation results showed that the pressure and velocity of the electrolyte in the IEG were oscillated by additional motion of cathodic tool. Additionally, the rotary combined US and ECM had better ability of making small holes than that of rotary ECM. Jia et al. [54] used the FEM to calculate the flow field distribution in ordinary ECM method of multiple slots with low-frequency tool vibrations.

Statistical methods have been adopted by many researchers recently. In this respect, Goel and Pandey [50] conducted statistical analysis for the MRR and hole taper using analysis of variance (ANOVA) and concluded that combining US vibrations to the electrolyte jet, resulted in the improvement of MRR and the reduction in the hole taper. Ebeid and coworkers [35] used the response surface methodology (RSM) for deriving mathematical models to describe the effect of applied voltage (12–24 V), feed rate (0.6–1.4 mm/min), back pressure, and vibration amplitude on the overcut and conicity of drilled holes. Jadhav et al. [36] used Taguchi technique to optimize the process parameters for maximum MRR and minimum overcut in US-assisted drilling of Inconel 60 alloy. Ayyappan et al. [37] developed a mathematical model correlating MRR and the surface roughness parameter  $Ra$  with machining conditions such as the gap voltage and electrolyte concentration for low-frequency vibrating tool assisted by a magnetic flux as an efficient hybrid technique in ECM.

## 8 Summary

VA-ECM is an alternative machining method that replaces the traditional ECM. From the literature review, the following points can be raised:

1. The use of vibration enhances the flushing of the machining products from the IEG and stops the formation of the passive oxide layer on the anodic surface. Hence MRR and the surface quality are improved.

2. For high accuracy in micromachining applications, nanosecond pulsed voltage together vibration assistance is recommended. Short pulses cause a high localization of the electrochemical dissolution action
3. For high efficiency and better machining stability of VA-ECM, abrasives can be mixed with the electrolyte
4. Using the magnetic flux assistance to VA-ECM increases the current density, MRR, and surface roughness.
5. USECM is suitable for machining materials that form a passivating layer over the anodic surface during normal ECM. Such a layer is successfully removed by using the US vibration
6. VA-ECM is recommended for micromachining applications at low frequency of vibration.
7. Adding US vibration to the flowing electrolyte improves surface finish and decreases hole taper.
8. US jet drilling by ECM raises the MRR and process accuracy and improves the surface quality.
9. The use of low-frequency vibration with ribbed wire and adding abrasive powder to the electrolyte improve the surface quality in VA-WECM.
10. Due to the complex mixture in the interelectrode gap, CFD and FEM methods are adopted for understanding the process behavior and quantifying the electrolyte flow effects.

## 9 Outlook

There are many critical points, faced by researchers during the application of VA-ECM. Further efforts are, therefore, to be made in the following directions:

1. The effect of VA-ECM process variables on the machinability of materials that form a passivating layer.



2. Investigating the percentage contribution of using vibrations and pulsed voltage on MRR, improvement of accuracy and reduction of surface roughness.
3. Using electrolyte mixtures that reduce the possibility of forming passive oxide layer during ECM.
4. The effect of vibration assistance in the case of hybrid ECM processes such as electrochemical grinding and electrochemical honing.
5. Modeling, simulation, and experimental study for VA-ECM assisted by abrasive powder or a magnetic flux.
6. Optimization of the process parameters using artificial neural network (ANN), fuzzy logic (FL), genetic algorithms (GA), grey relational analysis (GRA), artificial bee colony (ABC), multi-objective optimization, and simulation annealing (SA).

### Compliance with ethical standards

**Conflict of interests** The author declares that there is no conflict of interest.

### References

1. Rajurkar KP, Zhu D (1999) Improvement of electrochemical machining accuracy by using orbital electrode movement. *CIRP Ann Manuf Technol* 48(1):139–142. [https://doi.org/10.1016/s0007-8506\(07\)63150-3](https://doi.org/10.1016/s0007-8506(07)63150-3)
2. Rajkumar KP, Poovazhagan L, Saravanamuthukumar P, Javed Syed Ibrahim S, Santosh S (2015) Abrasive assisted electrochemical machining of Al-B<sub>4</sub>C nanocomposite. *Appl Mech Mater* 787:523–527. <https://doi.org/10.4028/www.scientific.net/amm.787.5>
3. Davydov AD, Volgin VM, Lyubimov VV (2004) Electrochemical machining of metals: fundamentals of electrochemical shaping. *Russ J Electrochem* 40(12):1230–1265. <https://doi.org/10.1007/s11175-005-0045-8>
4. Rajurkar KP, Kozak J, Wei B, McGeough JA (1993) Study of pulse electrochemical machining characteristics. *CIRP Ann Manuf Technol* 42(1):231–234
5. Rajurkar KP, Wei Kozak J, McGeough JA (1995) Modeling and monitoring interelectrode gap in pulse electrochemical machining. *CIRP Ann Manuf Technol* 44(1):177–180
6. Skoczypiec S (2016) Discussion of ultrashort voltage pulses electrochemical micromachining: a review. *Int J Adv Manuf Technol* 87(1–4):177–187. <https://doi.org/10.1007/s00170-016-8392-z>
7. Kumar P, Jadhav P, Beldar M, Jadhav DB, Sawant A (2018) Review paper on ECM, PECM and ultrasonic assisted PECM. *Mater Today Proc* 5:6381–6390
8. Kock M, Krichner V, Schuster R (2003) Electrochemical micromachining with ultrashort voltage pulses a versatile method with lithographical precision. *Electrochim Acta* 48:3213–3219
9. Maurer JJ, Mallett JJ, Hudson JL, Fick SE, Moffat TP, Shaw GA (2010) Electrochemical micromachining of Hastelloy B-2 with ultrashort voltage pulses. *Electrochim Acta* 55(3):952–958. <https://doi.org/10.1016/j.electacta.2009.09.004>
10. Liu Z, Zhang H, Chen H, Zeng Y (2013) Investigation of material removal rate in micro electrochemical machining with lower frequency vibration on workpiece. *Int J Mach Mach Mater* 14(1):91. <https://doi.org/10.1504/ijmmm.2013.055131>
11. Feng W, Jianshe Z, Dingming L, Yantao F, Zongjun T (2018) Experimental research on electrochemical machining of an arc-shaped slot array. *Int J Electrochem Sci* 13:9466–9480. <https://doi.org/10.20964/2018.10.12>
12. Skoczypiec S (2011) Research on ultrasonically assisted electrochemical machining process. *Int J Adv Manuf Technol* 52:565–574. <https://doi.org/10.1007/s00170-010-2774-4>
13. Perusich SA, Alkire RC (1991) Ultrasonically induced cavitation studies of electrochemical passivity and transports mechanisms. I Theoretical. *J Electrochem Soc* 138(3):700–707
14. Perusich SA, Alkire RC (1991) Ultrasonically induced cavitation studies of electrochemical passivity and transport mechanisms II. Experimental. *J Electrochem Soc* 138(3):708–713
15. Ruszaj A, Zybura M, Żurek R, Skrabalak G (2003) Some aspects of the electrochemical machining process supported by electrode ultrasonic vibrations optimization. *Proc Inst Mech Eng B J Eng Manuf* 217(10):1365–1371. <https://doi.org/10.1243/095440503322617135>
16. Ruszaj A, Skoczypiec S, Czekaj J, Miller T, Dziedzic J (2007) Surface micro and nanofinishing using pulse electrochemical machining process assisted by electrode ultrasonic vibrations. 15<sup>th</sup> International Symposium on Electromachining., Pittsburgh, Pennsylvania, USA, 6p
17. Skoczypiec S (2018) Electrochemical methods of micropart's manufacturing. In: Gupta K (ed) *Micro and precision manufacturing, engineering materials*. Springer International Publishing AG. [https://doi.org/10.1007/978-3-319-68801-5\\_2](https://doi.org/10.1007/978-3-319-68801-5_2)
18. Hewidy MS, Ebeid SJ, Rajurkar KP, El-Safti MF (2001) Electrochemical machining under orbital motion conditions. *J Mater Process Technol* 109(3):339–346. [https://doi.org/10.1016/s0924-0136\(00\)00827-x](https://doi.org/10.1016/s0924-0136(00)00827-x)
19. Sadollah Z, El-Hofy H (2002) Orbital electrochemical machining of electro-discharge machined surfaces, AMST '02 Conference, Udine, Italy, June 2002: 457–464
20. Paczkowski T, Zdrojewski J (2017) Monitoring and control of the electrochemical machining process under the conditions of a vibrating tool electrode. *J Mater Process Technol* 244:204–214. <https://doi.org/10.1016/j.jmatprotec.2017.01.023>
21. Fang X, Qu N, Zhang Y, Xu Z, Zhu D (2014) Effects of pulsating electrolyte flow in electrochemical machining. *J Mater Process Technol* 214(1):36–43. <https://doi.org/10.1016/j.jmatprotec.2013.07.012>
22. Zeng Y, Fang X, Zhang Y, Qu N (2014) Electrochemical drilling of deep small holes in titanium alloys with pulsating electrolyte flow. *Adv Mech Eng* 6:167070. <https://doi.org/10.1155/2014/167070>
23. Jiang X, Liu J, Qu N (2018) Electrochemical machining multiple slots of bipolar plates with tool vibration. *Int J Electrochem Sci* 13: 5552–5564. <https://doi.org/10.20964/2018.06.62>
24. Ghoshal B, Bhattacharyya B (2015) Investigation on profile of microchannel generated by electrochemical micromachining. *J Mater Process Technol* 222:410–421. <https://doi.org/10.1016/j.jmatprotec.2015.03.02538>
25. Ghoshal B, Bhattacharyya B (2015) Vibration assisted electrochemical micromachining of high aspect ratio micro features. *Precis Eng* 42:231–241. <https://doi.org/10.1016/j.precisioneng.2015.05.005>
26. Ghoshal B, Bhattacharyya B (2014) Shape control in micro bore-hole generation by EMM with the assistance of vibration of tool. *Precis Eng* 38(1):127–137. <https://doi.org/10.1016/j.precisioneng.2013.08.004>
27. Yang I, Park MS, Chu CN (2009) Micro ECM with ultrasonic vibrations using a semi-cylindrical tool. *Int J Precis Eng Manuf* 10(2):5–10. <https://doi.org/10.1007/s12541-009>
28. Feng Z, Granda E, Hung W (2016) Experimental investigation of vibration-assisted pulsed electrochemical machining. *Procedia Manuf* (5):798–814. <https://doi.org/10.1016/j.promfg.2016.08.065>



29. Kurogi S, Natsu W, Yu Z (2012) Investigation of machining characteristics of ultrasonic vibration assisted ECM. *Appl Mech Mater* (217-219):2555–2559. <https://doi.org/10.4028/www.scientific.net/AMM.217-219.2555>
30. Wang J, Chen W, Gao F, Han F (2014) Ultrasonically assisted electrochemical micro drilling with sidewall-insulated electrode. *Proc IMechE B J Eng Manuf* 230:1–9. <https://doi.org/10.1177/0954405414555740>
31. Wu Z, Wu X, Lei JXB, Jiang K, Zhong J, Diao D, Ruan S (2018) Vibration-assisted micro-ECM combined with polishing to machine 3D microcavities by using an electrolyte with suspended B<sub>4</sub>C particles. *J Mater Process Technol* (255):275–284. <https://doi.org/10.1016/j.jmatprotec.2017.12.025>
32. Wang M, Zhang Y, He Z, Peng W (2016) Deep micro-hole fabrication in EMM on stainless steel using disk micro-tool assisted by ultrasonic vibration. *J Mater Process Technol* 229:475–483. <https://doi.org/10.1016/j.jmatprotec.2015.10.004>
33. Patel JB, Feng Z, Villanueva PP, Hung WNP (2017) Quality enhancement with ultrasonic wave and pulsed current in electrochemical machining. *Procedia Manuf* 10:662–673. <https://doi.org/10.1016/j.promfg.2017.07.013>
34. Natsu W, Nakayama H, Yu Z (2012) Improvement of ECM characteristics by applying ultrasonic vibration. *Int J Precis Eng Manuf* 13(7):1131–1136. <https://doi.org/10.1007/s12541-012-0149-5>
35. Ebeid SJ, Hewidy MS, El-Taweel TA, Youssef AH (2004) Towards higher accuracy for ECM hybridized with low-frequency vibrations using the response surface methodology. *J Mater Process Technol* 149:432–438. <https://doi.org/10.1016/j.matprotec.2003.10.046>
36. Jadhav DB, Jadhav PV, Bilgi DS, Sawant AA (2018) Experimental investigation of MRR on inconel 600 using ultrasonic assisted pulse electrochemical machining. *International Conference on Mechanical, Materials and Renewable Energy IOP Conf Series: Materials Science and Engineering* 377 012095. <https://doi.org/10.1088/1757-899X/377/1/012095>
37. Ayyappan S, Sivakumar K, Kalaimathi M (2015) Electrochemical machining of 20MnCr5 alloy steel with magnetic flux assisted vibrating tool. *Proc Inst Mech Eng C J Mech Eng Sci* 231(10):1956–1965. <https://doi.org/10.1177/0954406215623310>
38. Hewidy MS, Ebeid SJ, El-Taweel TA, Youssef AH (2007) Modeling the performance of ECM assisted by low frequency vibrations. *J Mater Process Technol* 189(1-3):466–472. <https://doi.org/10.1016/j.jmatprotec.2007.02.032>
39. Liu ZX, Kang M, Fu XQ (2013) Simulation research of small holes by combined ultrasonic and electrochemical machining based on CFX. *Key Eng Mater* 584:60–66. <https://doi.org/10.4028/www.scientific.net/kem.584.6>
40. Zou X, Fang X, Chen M, Zhu D (2018) Investigation on mass transfer and dissolution localization of wire electrochemical machining using vibratory ribbed wire tools. *Precis Eng* 51:597–603. <https://doi.org/10.1016/j.precisioneng.2017.10.015>
41. Xu K, Zeng Y, Li P, Zhu D (2017) Vibration assisted wire electrochemical micro machining of array micro tools. *Precis Eng* 47:487–497. <https://doi.org/10.1016/j.precisioneng.2016.10.004>
42. Qu NS, Ji HJ, Zeng YB (2014) Wire electrochemical machining using reciprocated traveling wire. *Int J Adv Manuf Technol* 72: 677–683. <https://doi.org/10.1007/s00170-014-5704-z>
43. Fang XL, Zou XH, Chen M, Zhu D (2017) Study on wire electrochemical machining assisted with large-amplitude vibrations of ribbed wire electrodes. *CIRP Ann* 66(1):205–208. <https://doi.org/10.1016/j.cirp.2017.04.135>
44. Jiang K, Wu X, Lei J, Wu Z, Wu W, Li W, Diao D (2018) Vibration-assisted wire electrochemical micromachining with a suspension of B<sub>4</sub>C particles in the electrolyte. *Int J Adv Manuf Technol* 97(9-12): 3565–3574. <https://doi.org/10.1007/s00170-018-2190-8>
45. Wang S, Zhu D, Zeng Y, Liu Y (2010) Micro wire electrode electrochemical cutting with low frequency and small amplitude tool vibration. *Int J Adv Manuf Technol* 53(5–8):535–544. <https://doi.org/10.1007/s00170-010-2835-8>
46. Kim US, Park JW (2013) Vibration-assisted electrochemical polishing for extremely smooth surface generation. *Adv Mater Res* 813:475–478. <https://doi.org/10.4028/www.scientific.net/AMR.813.475>
47. Pa PS (2008) Design of finish-tool in ultrasonic electrochemical finishing processes. *Mater Manuf Process* 23(5):457–462. <https://doi.org/10.1080/10426910802103528>
48. Ghoshal B, Bhattacharyya B (2013) Influence of vibration on micro-tool fabrication by electrochemical machining. *Int J Mach Tools Manuf* 64:49–59. <https://doi.org/10.1016/j.ijmactools.2012.07.014>
49. Skoczypiec S (2007) Numerical investigations on ultrasonically assisted electrochemical machining process (USECM) 15th International Symposium on Electromachining. (ISEM XV)
50. Goel H, Pandey PM (2017) Experimental investigations into the ultrasonic assisted jet electrochemical micro-drilling process. *Mater Manuf Process* 32(13):1547–1556. <https://doi.org/10.1080/10426914.2017.1279294>
51. Nicoară D, Hedeş A, Şora I (2006) Ultrasonic enhancement of an electrochemical machining process. *Proceedings of the 5th WSEAS International Conference on Applications of Electrical Engineering, Prague, Czech Republic, March 12-14:213-218*
52. Xu L, Pan Y (2014) Electrochemical micromachining using vibrating tool electrode. *Int J Adv Manuf Technol* 75:645–650. <https://doi.org/10.1007/s00170-014-6156-1>
53. Wang M, Zhang Y, Xu X, Chen G, Clare AT, Ahmed N (2018) Effects of tool intermittent vibration on helical internal hole processing in electrochemical machining. *Proc Inst Mech Eng C J Mech Eng Sci* 233:1–10. <https://doi.org/10.1177/0954406218792591>
54. Jia L, Xiaochen J, Di Z (2016) Electrochemical machining of multiple slots with low-frequency tool vibrations. *Procedia CIRP* 42: 799–803. <https://doi.org/10.1016/j.procir.2016.02.322>
55. Mitchell-Smith J, Clare AT (2016) Electrochemical jet machining of titanium: overcoming passivation layers with ultrasonic assistance. *Procedia CIRP* 42:379–383. <https://doi.org/10.1016/j.procir.2016.02.215>

**Publisher's note** Springer Nature remains neutral with regard to jurisdictional claims in published maps and institutional affiliations.